Properties and manufacturing of a new starch plastic

de Graaf, R.A.; Janssen, L.P.B.M.

Published in:
Polymer Engineering and Science

DOI:
10.1002/pen.10755

Properties and Manufacturing of a New Starch Plastic

R. A. DE GRAAF* *and* L. P. B. M. JANSSEN

Department of Chemical Engineering
The University of Groningen
Nijenborgh 4, 9747 AG, Groningen, The Netherlands

Environmental awareness has strongly stimulated the introduction of biodegradable materials based on renewable resources of natural origin. This paper describes the properties and manufacturing of such a bioplastic. In a counter-rotating twin screw extruder, starch and polystyrene were mixed. To enhance material properties such as tensile strength and impact strength, two routes were followed. First, the starch was altered by grafting polystyrene onto the starch backbone using a counter rotating twin screw extruder. The newly formed material was blended with polystyrene in different ratios. Tensile strengths of 10 to 35 MPa were obtained while notched impact strengths varied from 0.5 J m^{-1} to 1.5 J m^{-1}. Soaking the material for a certain time in water and measuring the tensile strength of the wet material revealed that the tensile strength remained more the less the same for blends containing more than 30 wt% PS. Second, polystyrene grafted starch was used as a compatibilizer. A homogenous blend could be obtained (according to scanning electronic microscopy pictures) by adding the compatibilizer to a starch, polystyrene, and water mixture. Again, tensile and impact strengths were measured for different ratios of the polymers used. The tensile strength and the impact strength were of the same magnitude as they were with the blended material. X-ray diffraction and DSC measurements revealed a highly ordered system. When the fraction of polystyrene was above 60 wt% of the blend, the amylose part of the starch crystallized.

INTRODUCTION

Food applications of starches have a long-standing tradition. They require a continuous process with high production rates, a long shelf life and (often) a low density. Extruders, especially, have gained a considerable share of the market for food production machinery. Typical examples of extruded foods are snacks, toast, pasta, breakfast cereals, pet food and candy. The scope in products demonstrates the versatility in operating possibilities an extruder offers. Snacks, for instance, are processed at high shear, high temperature and a low moisture content in order to degrade the starch for easier digestibility. Breakfast cereals, on the other hand, are processed at low shear, high temperature and a high moisture contents in order to retain the firm structure that we are accustomed to at breakfast.

Starch is the basis of various chemicals. Therefore, the starch can be modified to obtain specific properties. A well-known example of a modification reaction is the benzylation of starch to make it slightly hydrophobic. Benzylated starch is used in paper coating and in the textile industry for pre-treating of yarn. A recent application of starch in the non-food sector is its use as packaging material. Until now, three different applications have been known:

- Starch is used as filler in synthetic polymers.
- Starch is blended on a micro-scale with synthetic polymers.
- Starch is mixed with polyoles to form a thermoplastic amorphous mass.

It is obvious that in these three applications the biodegradability increases in the order mentioned above.

The simplest way to use starch as packaging material is as a filler for synthetic polymers. The starch is physically blended with synthetic polymers, but it remains in the form as separate conglomerates in the polymeric matrix, the size of the conglomerates being a function of the interfacial energy between starch and plastic and the shear history during the process. The advantage of this method is that the thickness of the packaging material increases and that starch is relatively cheap. Although these combined materials

*Corresponding author: Robbert de Graaf, Department of Chemical Engineering, Groningen University, Nijenborgh 4, 9747 AG, Groningen, (phone) +31 50 3634462, (fax) +31 50 3634479, (e-mail) R.A.de.Graaf@chem.rug.nl.

are sometimes claimed to be partially biodegradable, it is clear that if the encapsulated starch cannot be reached by micro-organisms, the biodegradability is very questionable. Moreover, even if the starch would be degraded, the matrix of the remaining synthetic polymer is so strong and thick that it will not degrade within a foreseeable time. In order to make the starch-plastic combination more biodegradable, size reduction of the plastic phase is required. This can be obtained in two ways:

- Physically, by rigorous application of high shear forces in combination to a substantial decrease in interfacial tension between starch and plastic, which will lead to a micro scale blending. The starch must form a semi-continuous phase in order to make it accessible to micro-organisms. After the degradation of the starch, the surface to volume ratio of the remaining synthetic polymer is so large that also this polymer may degrade.
- By chemical bonding, where block-copolymers of starch and synthetic polymer are formed.

The third category of starch based packaging materials consists of a mixture of pure starch and polyoles like glycerol and sorbitol. No synthetic polymers are involved. This mixture forms an amorphous mass after processing that can been formed into films, sheets and trays. The polyol serves as an internal lubricant for the starch and prevents retrogradation. In this study, polystyrene grafted starch (PS-g-starch) (1) was blended with polystyrene and starch in order to obtain a new polymer that can be used, for instance, as a packaging material. First the starch was modified by grafting polystyrene onto the starch backbone (2, 3). The newly formed material was blended with polystyrene using different process conditions. Beside the chemical properties of the polymers used, physical parameters like volume fraction, molecular weight, viscosity ratio, interfacial tension and shear history are important factors determining the final blend properties (4–7). When these parameters are varied, material properties like water resistance and tensile and impact strengths can be altered. The amount of starch incorporated into the blend can be increased, when PS-g-starch is used as a compatibilizer. Again, physical parameters like volume fraction, molecular weight, viscosity ratio, interfacial tension and shear history are important factors determining the final blend properties.

THEORY

Blending Two or More Polymers

Polymer mixtures can be divided into miscible or immiscible systems. For miscible systems, the behavior of a blend is similar to that of a homopolymer or a random copolymer. Tailor-made properties can be obtained simply by changing the volume fractions. It should be clear that PS and starch belong to the category of immiscible systems. Distributive and dispersive mixing mechanisms will determine the material properties like the polymer layer distribution, to a greater extend (8). The increase in interfacial area is given by: $A/A_o = \gamma_t \cos \alpha_o$, in which α_o is the initial angle between the stream lines and the normal vector of the contact area A, A_o is the initial area. Increased dispersive mixing results in the breakup of the formed polymer layers into droplets (4). In general, the material with the lowest viscosity or highest volume fraction will form the continuous phase. The following semi-empirical equation (9) predicts the mid-point of phase inversion.

$$\frac{\eta_1}{\eta_2} \cdot \frac{\varphi_2}{\varphi_1} \approx 1 \tag{1}$$

in which η is the viscosity and φ is the volume fraction. At low volume fractions, the breakup of the dispersed phase into droplets has been studied extensively in well-defined flow fields (10–13). The droplets undergo continuous deformation, resulting in long threads. The stability of these drops is dependent on the viscosity ratio (12):

$$\Psi = \frac{\eta_d}{\eta_c} \tag{2}$$

and of the ratio of the applied shear stress and the interfacial tension, the capillary number:

$$Ca = \frac{\eta_c \dot{\gamma} d}{\nu_{12}} \tag{3}$$

in which η is the viscosity of the continuous (subscript c) phase, ν is the interfacial tension, $\dot{\gamma}$ is the shear rate and d is the droplet diameter.

Determining the Interfacial Tension Between PS and Starch

In the literature, no data exists on the interfacial tension between PS and starch. But with the help of a theory proposed by Wu (14), an estimate of this property can be made. Wu proposes an equation, based on "reciprocal" mean and force additivity, to calculate the interfacial tension between polymers or between a polymer and an ordinary liquid:

$$\nu_{12} = \nu_1 + \nu_2 - \frac{4\nu_1^d \nu_2^d}{\nu_1^d + \nu_2^d} - \frac{4\nu_1^P \nu_2^P}{\nu_1^P + \nu_2^P} \tag{4}$$

where ν_{12} is the interfacial tension, ν_i the surface tension; ν_i^d and ν_i^P the dispersion and the polar components of ν_i, respectively. According to Wu, the interfacial tension arises mainly from disparity in the polarities of the two phases. Assuming that the starch polymers are perfectly mixed with the water, the interfacial tension primarily exists between PS and water. From (15) tension data (surface and interfacial) as a function of the temperature were taken. Using these values the interfacial tension between PS and water

was calculated to be 37×10^{-3} N m^{-1}. The value of the interfacial tension existing between PS and polyethylene (both very apolaric materials) is 8.3×10^{-3} N m^{-1} at 20°C and 5.1×10^{-3} N m^{-1} at 180°C (14). It is assumed that the interfacial tension between PS and grafted PS is considerably smaller.

Determining the Viscosity of Starch and PS

An important aspect is the influence of the viscosity. Usually, non-Newtonian flow behavior of starchy materials is to be expected. Not only the starch materials but also the chemical reactions performed with these materials have influence on the viscosity function. In our case a viscosity function was derived describing the behavior of concentrated starch pastes (16).

In the case of a concentrated starch paste, the viscosity is a function of strain, strain history, temperature and the amount of water. The strain history W(t) is introduced into the viscosity equation using an exponential dependency of the apparent viscosity on the amount of work performed on the paste:

$$W(t) = \frac{1}{\rho_p w_{starch}} \int_0^t \eta(t)\dot{\gamma}\, dt \; [kJ\, kg^{-1}\, dry\ starch] \quad (5)$$

The viscosity equation is a modified version from that presented by van Zuillichem *et al.* (17) and Dolan and Steffe (18) and reads:

$$\eta_{app} = \eta_0 e^{\left\{\frac{A}{T} + Bw_{starch} - CW(t) + (n-1)\ln\dot{\gamma}\right\}} \quad (6)$$

here η_0, A, B, C and n are fit parameters coming from measurements, w_{starch} is the amount of pure starch in the gel, $\dot{\gamma}$ is the shear rate and T the temperature of the gel. The fit parameters have been measured by Lammers *et al.* (16). *Figure 1* shows the viscosity of starch at moisture contents below 30% and temperatures above 150°C. *Equation 6* was used to calculate these values. These temperatures have to be that high in order to obtain a good PS melt. Temperatures above the 180°C result in degradation of starch and should thus be avoided. It should be noted that the starch viscosity function has been verified only for a temperature of 343.15 K and starch concentration of up to 0.4 kg starch/kg water. Thus the calculated apparent viscosity may be wrong. The viscosity of PS has been measured in a Cone and plate viscometer using different temperatures and shear rates as used in the experiments.

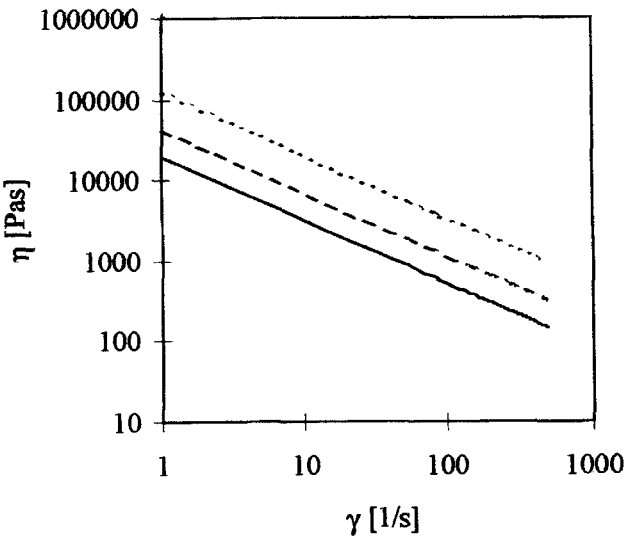

Fig. 1. Apparent viscosity as a function of the shear rate for potato starch. w_{starch} = 0.7, · · T = 60°C, – – T = 90°C, —— T = 160°C.

Total Shear in a Counter Rotating Twin Screw Extruder

A very important parameter determining the mixing between polymers is the shear. In a counter rotating twin screw extruder, two shear areas can be detected—a low shear region in the chambers and a high shear region in the leakage gaps. In comparison with other types of extruders, many counter rotating machines have deeply cut channels and low rotational speeds. This implies that a fluid element, during the major part of its residence time in the fully filled zone, is subjected to a shear that is considerably lower than in other types of extruders. Typical values for the shear in the chambers and the leakage gaps of the used extruder are 2 s^{-1} and 70 s^{-1} respectively. These values are of course dependent on the screw speed and the geometry of the screw. Given the viscosity, the interfacial tension and the shear values the Ca number during the processing time can be predicted. Two shear boundaries are present. The lowest shear boundary is formed by material only exposed to low shear rates (19). This material has the shortest residence time because it remains in a single chamber without leaking back. The mean residence time (20) in a single fully filled chamber (m flighted screw) is equal to:

$$\tau_{chamber} = \frac{2mV_c}{Q_{leak}} \quad (7)$$

in which Q_{leak} is the leakage flow, m = 2 and V_c the C-shaped chamber (6.7×10^{-6} m^3). At a screw speed of 20 RPM and a die resistance of 4×10^{-13} m^3, the leakage flow is about 6.9×10^{-6} m^3 resulting in a mean residence time in the chambers of about: 4 s.

The total shear in one chamber imposed on the material is equal to:

$$\gamma_{total,\ chamber} = \tau_{chamber}\dot{\gamma}_{chamber} = 4*2 = 8s^{-1} \quad (8)$$

The highest shear boundary line is formed by material, which has leaked several times through the leakage gaps and was thus subjected to a higher shear level. The residence time of this material was the longest. In this case the subscript "chamber" in *Eq 8* has to be replaced by "gap" to obtain the total shear imposed on the material in the leakage gaps. The residence time

in the leakage gaps is equal to: $\tau_{leak,gap} = V_{leak,gap}/\dot{Q}_{v,leak}$. In our case the extruder used has a total leakage volume of 1.68×10^{-6} m^3 ($V_{C\text{-}chamber} = 6.7 \times 10^{-6}$ m^3). Together with the data presented above, the mean residence time in the leakage gaps is about 0.25 s, giving a total shear of 17.5 s^{-1}. Using these two shear levels, the average shear imposed on an average fraction of the material equals:

$$\bar{\gamma} = \tau_{MRT}[(1 - \alpha)\dot{\gamma}_{chamber} + \alpha\dot{\gamma}_{gap} \quad (9)$$

in which α is the total volume fraction in the fully filled zone occupied by the leakage gaps. At 160°C and a shear of 2 s^{-1}, the viscosity of 70 wt% starch (30 wt% water) is about 3500 Pa s. Its viscosity drops to 550 Pa s when the shear increases to 70 s^{-1}. In the case of polystyrene, the viscosity drops from 2500 to 90 Pa s. The viscosity ratio is thus 0.7 and 0.16 for γ = 2 to 70 s^{-1}, respectively. Assuming an initial granule size (PS) of 3 mm, the Ca number becomes 567 at γ = 2 s^{-1}, increasing to Ca = 3121 for shear rates of 70 s^{-1}. In both shear regimes, the viscosity ratio is smaller than 1, while the initial Ca-number $\gg$ 1. According to Grace (12), these Ca -numbers exceed the Critical Ca numbers required for breakup. The mean residence time in the fully filled chambers is equal to 116 s, giving a average total shear of: 1020 s^{-1}. The breakup times in the leakage gaps are generally to short to let a thread break up (14). Assuming no reorientation, a droplet with an initial diameter (a) of 3 mm is deformed into a thread with diameter B:

$$B = a(1 + \gamma^2)^{-1/4} \approx 60\,\mu m \quad (10)$$

In the case of reorientation, this value will be lower.

Graft Copolymers

In order to stabilize the morphology formed (21), graft and block copolymers A-B may act as emulsifiers in a system containing the immiscible polymers A and B (22). The copolymers tend to concentrate at the interface, promoting interactions between the two phases. Finer dispersions and improved mechanical properties are the result. Thomas *et al.* (23) show that two limiting cases can be chosen in order to achieve the optimal blend. Either a relatively high concentration of a small molecular weight copolymer (M_w copolymer > M_w homopolymer) can be selected, or a small amount of a high molecular weight block copolymer can be used. Assuming that the same argument concerning block-copolymers can be applied to graft copolymers, it is important to create graft copolymers with high molecular weights or high graft percentages (21, 24, 25).

EXPERIMENTAL

The grafted material was produced as described in (3). Two material types were produced, with MAH (maleic anhydride) and without MAH. The type without MAH had a lower graft percentage and PS content, while the molecular weight of the grafted PS branches is higher. During these experiments a counter rotating closely intermeshing twin-screw extruder (24) was used with a screw diameter of 50 mm, an L/D of 6 and a flight gap of 1.0 mm. The screw speed was 30 RPM, $\dot{Q}_{styrene}$ = 3 g min^{-1}, $\dot{Q}_{starch}$ = 30 g min^{-1}, $\dot{Q}_{H2O}$ = 3.5 g min^{-1}. After preheating the extruder, a mixture of starch, water with c_{K2S2O8} = 2.5 wt%, styrene, benzoylperoxide (BPO) (c_{BPO} = 2 mol%) and 20 mol% MAH (only in the case of producing MAH-co-PS-g-starch) was fed to the extruder. The starch contained about 15 wt% water. Samples were taken when a stable temperature and pressure profile along the extruder was obtained. In this way, enough material could be made for the blending experiments. This material was ground until granules of 2–3 mm were obtained.

The same extruder was used for the blend experiments. A different temperature profile was used in order to obtain a good melt of PS, starch and additives. In the hopper zone; PS, starch and the compatibilizer were added; water was added in the first heating zone in order to gelatinize the starch. The blended material was ground again until granules of 2–3 mm were obtained. In *Tables 1, 2* and *3* the extruder settings are given. The potato starch was obtained from AVEBE. Three polystyrene grades from Shell Holland were used (PS 2000, PS 5000 and PS 7000).

The analyzing techniques Scanning Electronic Microscopy (SEM), Transmission Electronic Microscopy (TEM), Differential Scanning Calorimetry (DSC), and X-ray scattering were used. In the case of SEM, samples were quenched in liquid nitrogen and then broken to the right size. The sample was coated with gold before scanning. The maximum acceleration energy used was 29 KV. Higher values resulted in deterioration of the sample. Samples used in TEM were first microtomed (dry) in order to obtain slices of 0.1 μm. The obtained coupes were placed inside a copper net. X-ray diffractions were taken of thin slices of material placed at different angles relative to the X-rays. The exposure of the material to the X-rays was 1.5 h. In this way it could be determined if the material was amorphous or crystalline. From experiments with DSC, information about the amorphous structure was obtained. The DSC used was of the type "Gold" manufactured by Polymer Laboratories. Tensile strengths (ASTM D1705) and Notched Izod notch tests were used for determining the material properties and blend characteristics. Compression molding made test samples for the tensile strength and Izod notch test. The temperature of the used press was 145°C, the pressure was 40 tons, the heating time was 20 minutes, and the cooling was 10 minutes. The tensile strength of a sample was determined with a Instron testing system 1.09. The crosshead speed was 10 mm min^{-1} and the sample rate was 20 pts s^{-1}. The humidity was in all cases 50%, while the measuring temperature remained 20°C.

Table 1. Results of the Tensile Strength for Blends of PS and PS-g-Starch.

N°	w_{Starch} [–]	w_{PS} [–]	Tensile Strength [MPa]	Impact [J m^{-1}]
PS-g-Starch, 30 wt% H_2O towards starch, PS5000 N = 23 RPM, K = 2 × 10^{-11} m^3, T-prof = 90-160-170°C, Q_{in} = 48 g min^{-1}				
1	0	1.0	27.5	—
2	0.3	0.7	23.1	—
3	0.5	0.5	22.6	—
4	0.7	0.3	22.7	—
5	0.9	0.1	22.0	—
PS-g-Starch, 30 wt% H_2O towards starch, PS5000 N = 23 RPM, K = 2 × 10^{-11} m^3, T-prof = 90-160-170°C, Q_{in} = 48 g min^{-1}				
6	0.0	1.0	27.5	—
7	0.1	0.9	27.3	—
8	0.3	0.7	18.7	—
9	0.5	0.5	15.2	—
10	0.7	0.3	16.7	
11	1.0	0.0	15	
MAH-co-PS-g-Starch, 30 wt% H_2O towards starch, PS5000 N = 23 RPM, K = 2 × 10^{-11} m^3, T-prof = 90-160-170°C, Q_{in} = 48 g min^{-1}				
12	0	1.0	27.5	—
13	0.3	0.7	23.1	—
14	0.5	0.5	22.6	—
15	0.7	0.3	22.7	—
16	0.9	0.1	22.0	—
PS-g-Starch, 30 wt% H_2O towards starch, PS5000 N = 23 RPM, K = 2 × 10^{-11} m^3, T-prof = 90-160-170°C, Q_{in} = 48 g min^{-1}				
17	0.0	1.0	27.5	—
18	0.1	0.9	27.3	—
19	0.3	0.7	18.7	—
20	0.5	0.5	15.2	—
21	0.7	0.3	16.7	
22	1.0	0.0	15	

Table 2. Results of the Tensile Strength for Blends Between PS, PS-g-Starch and Water, When Soaked for a Certain Time in Water.

N°	time [min]	Tensile Strength [MPa]
PS-g-Starch, 30 wt% H_2O towards starch, PS5000 (2 wt%) N = 23 RPM, K = 2 × 10^{-11} m^3, T-prof = 90-160-170°C, Q_{in} = 48 g min^{-1}		
1	0.1	15.0
2	10	2.5
3	50	0.5
4	100	0.5
5	1330	0.1
PS-g-Starch, 30 wt% H_2O towards starch, PS5000 (30 wt%) N = 23 RPM, K = 2 × 10^{-11} m^3, T-prof = 90-160-170°C, Q_{in} = 48 g min^{-1}		
6	0.1	21.0
7	10	8.1
8	100	5.8
9	1000	3.9
PS-g-Starch, 30 wt% H_2O towards starch, PS5000 (50 wt%) N = 23 RPM, K = 2 × 10^{-11} m^3, T-prof = 90-160-170°C, Q_{in} = 48 g min^{-1}		
10	0.1	23.0
11	10	14.6
12	100	8.7
13	1000	10.9
PS-g-Starch, 30 wt% H_2O towards starch, PS5000 (70 wt%) N = 23 RPM, K = 2 × 10^{-11} m^3, T-prof = 90-160-170°C, Q_{in} = 48 g min^{-1}		
14	0.1	28.2
15	10	24.1
16	100	20.2
17	1000	21.3
PS-g-Starch, 0.3 wt% H_2O towards starch, PS5000 (90 wt%) N = 23 RPM, K = 2 × 10^{-11} m^3, T-prof = 90-160-170°C, Q_{in} = 48 g min^{-1}		
	0.1	30.8
	10	30.8
	60	30.5
	260	25.6
	370	27.3

RESULTS AND DISCUSSION

In general, material properties improve when the dispersion degree of the blended polymers increases. Detecting the dispersion degree can be done with SEM and TEM. SEM photos (*Fig. 2*) of the copolymer with and without MAH revealed a smooth surface, indicating good mixing. The surface changes from smooth to layered structures when the copolymer (30 wt%) with or without MAH is mixed with PS (*Fig. 3*); still, no phase separation is detected. The very open structure in *Fig. 3* is caused by the evaporation of water when the material leaves the extruder. In *Fig. 4*, the amount of the MAH copolymer mixed with PS is increased from 30 to 70 wt%. Again, no phase separation was detected.

Using the copolymer as a compatibilizer in a mixture of PS and starch (*Fig. 5*) revealed long slender PS threads with diameters of 10 μm and a maximum observed length of 100 μm (the continuous phase was starch, 50 wt%).

TEM was also performed (*Fig. 6* and *7*). Because of the laborious work of obtaining one TEM sample, only two mixtures were studied. The image of a mixture of 70 wt% PS and 30 wt% PS-g-starch (without MAH) revealed that in a matrix of PS, drops of about 2–4.1 μm of the copolymer were seen. The other mixture (65 wt% PS, 30 wt% starch and 5 wt% PS-g-starch (without MAH) revealed starch drops of 0.5 to 2 μm in a PS matrix.

With DSC and X-ray scattering, it was investigated whether the blends formed had an amorphous or crystalline structure. DSC curves show highly ordered structures. Almost all tested blends revealed an endothermic peak between 150°C and 200°C during the DSC measurements. Because the glass transition of PS is situated around 102°C and starch does not have

Table 3. Results of the Tensile Strength and Izod Notch Tests for the Compatibilizer Experiments (Starch, PS, PS-g-Starch or (MAH-co-)PS-g-Starch).

No	w_{Starch} [–]	w_{PS} [–]	$w_{Compatibilizer}$ [–]	Tensile Strength [MPa]	Impact Strength [J m^{-1}]
(MAH-co-)PS-g-Starch, 30 wt% H_2O towards starch, PS5000, Starch N = 16 RPM, K = 2 × 10^{-11} m^3, T-prof = 90-160-170°C, Q_{in} = 52 g min^{-1}					
1	0.495	0.495	0.01	16.9	—
2	0.475	0.475	0.05	22.0	—
3	0.450	0.450	0.10	20.1	—
4	0.425	0.425	0.15	20.9	—
5	0.400	0.400	0.20	24.0	—
PS-g-Starch, 30 wt% H_2O towards starch, PS5000, Starch N = 16 RPM, K = 2 × 10^{-11} m^3, T-prof = 90-160-170°C, Q_{in} = 52 g min^{-1}					
6	0.495	0.495	0.01	16.0	—
7	0.475	0.475	0.05	13.8	—
8	0.450	0.450	0.10	14.2	—
9	0.425	0.425	0.15	16.0	—
10	0.400	0.400	0.20	15.3	—
PS-g-Starch, 30 wt% H_2O towards starch, PS5000, Starch N = 16 RPM, K = 2 × 10^{-11} m^3, T-prof = 90-160-170°C, Q_{in} = 52 g min^{-1}					
11	0.75	0.13	0.049	23.4	0.52
12	0.70	0.18	0.049	28.9	0.39
13	0.60	0.22	0.049	24.4	0.45
14	0.53	0.36	0.049	30.7	0.63
15	0.36	0.55	0.049	30.5	0.73
16	0.25	0.64	0.049	30.9	0.64
17	0	0.95	0.049	31.9	0.75
PS-g-Starch, 30 wt% H_2O towards starch, PS5000, Starch N = 16 RPM, K = 2 × 10^{-11} m^3, T-prof = 90-160-170°C, Q_{in} = 52 g min^{-1}					
18	0.80	0.09	0.049	21.1	0.52
19	0.60	0.18	0.049	22.0	0.66
20	0.54	0.33	0.049	18.3	1.46
21	0.44	0.43	0.049	21.2	1.42
22	0.37	0.49	0.049	25.1	1.24
23	0.0	0.87	0.049	27.0	1.10
PS-g-Starch, 30 wt% H_2O towards starch, PS5000, Starch N = 16 RPM, K = 2 × 10^{-11} m^3, T-prof = 90-160-170°C, Q_{in} = 52 g min^{-1}					
24	0.75	0.13	0.049	28.9	—
25	0.70	9.18	0.049	22.8	0.41
26	0.60	0.22	0.049	27.0	0.79
27	0.53	0.36	0.049	26.8	0.78
28	0.36	0.55	0.049	29.6	1.09
29	0.25	0.64	0.049	27.4	1.26
30	0	0.95	0.049	30.5	1.08

a melt or glass-transition peak, a new structure is formed. X-ray scatter experiments show crystallinity in one case only (*Fig. 8*). In all other cases, diffuse rings due to the starch or PS were present. According to these experiments, we suggest that reorientation of amylose (lowest M_w of the used polymers) occurred during the blending of the polymers under high pressures (which are always present in the extruder). Examining the tensile strength reveals that the mixed MAH-co-PS-g-starch with PS is stronger than PS-g-starch mixed with PS (*Fig. 9* and *10*). *Figure 9* also reveals that an increased screw speed improves the blend until an optimum is reached. This optimum is caused by degradation of the starch which already starts at temperatures above 180°C. *Figure 10* shows that up to 70 wt% PS, the material properties remain the same, at higher PS weights, the tensile strength increases. Soaking these samples for some time in water (*Fig. 11*) reveals that at increasing PS weights, the blend becomes more water-resistant.

Examining the tensile strengths of blends where starch, PS and PS-g-starch are mixed reveal that an increased amount of compatibilizer (*Fig. 12*) gives higher tensile strengths. Again, MAH-co-PS-g-starch gave better results compared to PS-g-starch. Increasing the die temperature showed an optimum tensile

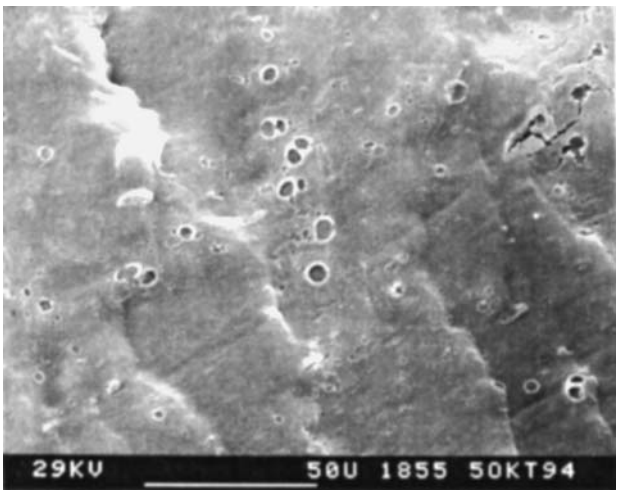

Fig. 2. SEM picture of PS-g-starch.

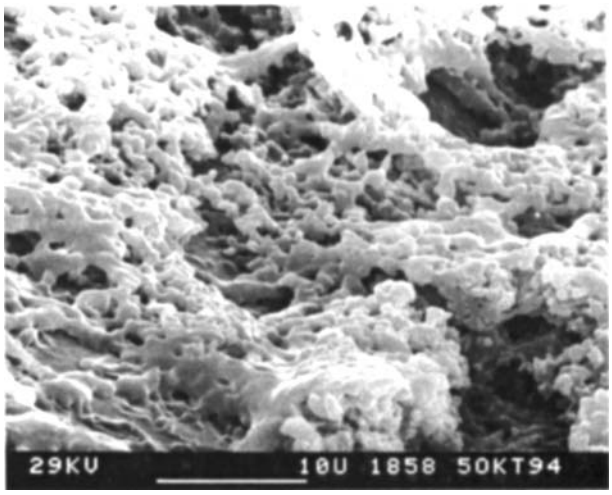

Fig. 4. SEM picture of 70 wt% MAH-co-PS-g-starch blended (30 wt% PS-5000).

strength of 27 MPa at 160°C, while at higher temperatures, the tensile strength decreases. As has been mentioned, the starch is destroyed at temperatures above 180°C, reducing the tensile strength.

In *Figs. 13* and *14*, the molecular weight of the polystyrene phase was changed. Three different molecular weights were used, namely 190, 220 and 300 kg mol^{-1} (polydispersity = 4 – 5). These PS grades were all mixed with PS-g-starch (in different ratios) and starch. The amount of compatibilizer remained the same. In the case of MAH-co-PS-starch, the M_w was about 249,672 while PS-g-starch had an M_w of 31,000.

The graft percentage of both MAH-co-PS-g-starch and PS-g-starch (60%) were almost the same (deviation of about ± 5%); this was also the case for the amount of homopolymer formed (about 10 ± 5%). *Figure 13* shows the results of the tensile strength as a function of the PS ratio in the blend for different molecular weights. This *Figure* clearly shows that the PS grade with the lowest molecular weight results in the highest tensile strengths. All PS grades show at PS ratios of 0.15 to 0.4 a dip in the tensile strength; at lower PS ratios, the tensile strength increases again. According to Heikens and Brentsen (24), the dispersed phase in blends where $\varphi_d > 0.15$ cannot be considered as dilute, resulting in co-continuous structures. These structures will emerge until finally a composition is reached at which phase inversion occurs. According to Bohm *et al.* (25), the lower viscosity or higher volume fraction will form the continuous phase. Using *Eq 1*, the mid-point of the inversion diagram can be predicted. Assuming that the starch viscosity is about 10 times the PS viscosity, the mid-point should occur at a ratio of about 10 wt% PS, which is indeed in the same area in which the dip in the measurements is obtained.

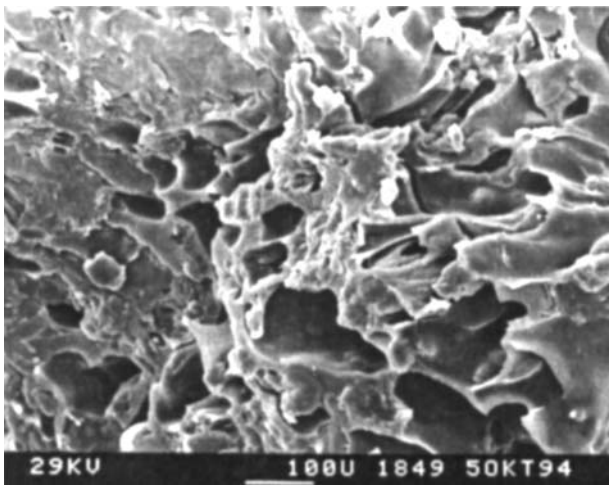

Fig. 3. SEM picture of 30 wt% PS-g-starch blended with 70 wt% PS-5000.

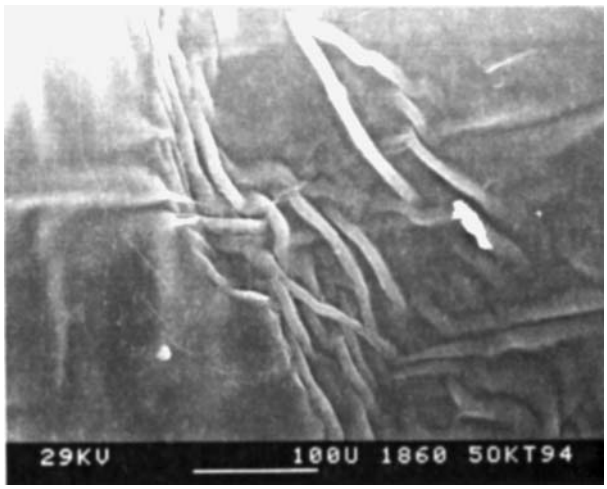

Fig. 5. SEM picture of 50 wt% starch blended with 25 wt% PS-g-starch (25 wt% PS-5000).

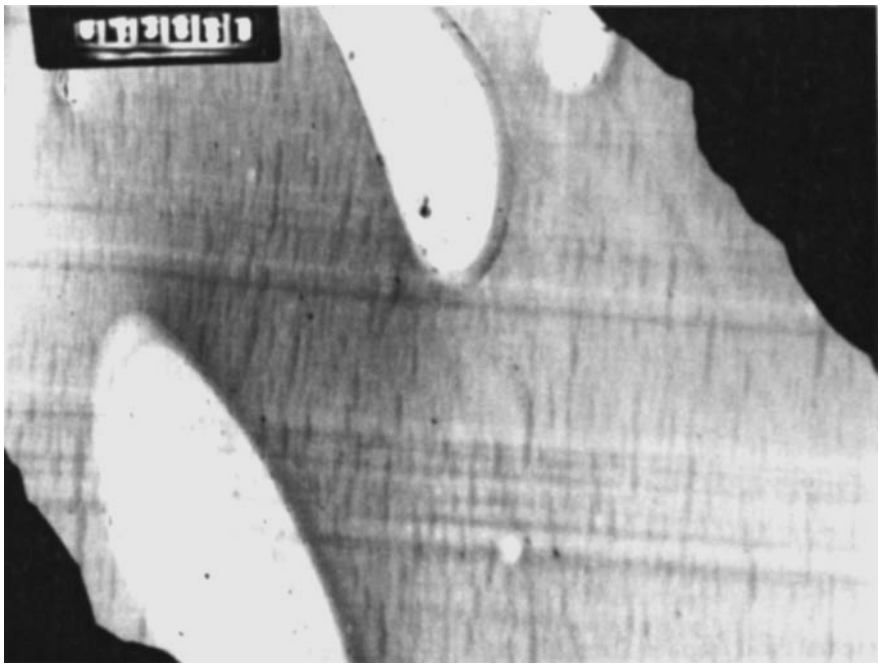

Fig. 6. TEM picture of 70 wt% PS 5000, 30 wt% PS-g-starch.

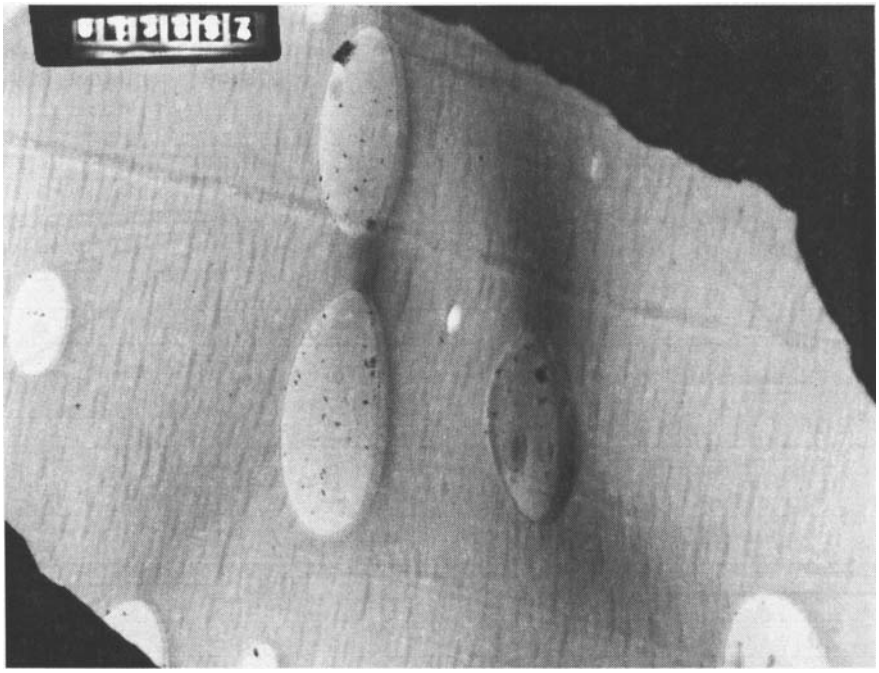

Fig. 7. TEM picture of 65 wt% PS-5000, 30 wt% starch and 5 wt% PS-g-starch.

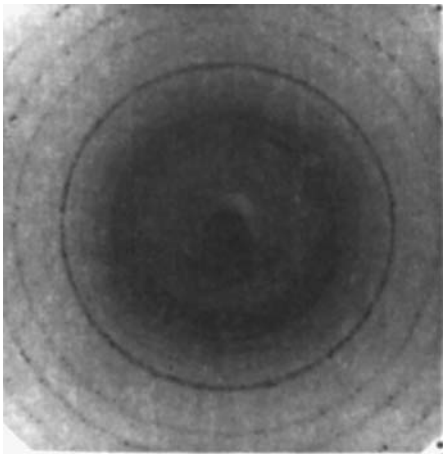

Fig. 8. X-ray scatter picture of 30 wt% PS-g-starch blended (70 wt% PS 5000).

In *Fig. 14*, the Notched Izod impact strength as a function of the PS ratio is presented. The impact strength is, for high PS contents, almost constant. Increasing starch fractions results in slightly decreasing impact strengths. This decreasing trend appears at the same area in which the change of tensile strength in *Fig. 13* is measured. So it is assumed again that at that area, phase inversion is occurring, giving rise to all kinds of discontinuous structures.

CONCLUSIONS

In this article the mixing of PS with PS-g-starch and pure starch is studied. All experiments reveal that reasonable blends can be obtained with tensile and Izod notch strengths of the same order as pure PS. Parameters such as the molecular weight, the processing conditions, and polymer ratios have their influence on the process. These influences can be predicted to some extent and show that high molecular weights of the graft copolymer are favorable. Analyzing techniques such as SEM, TEM, DSC and X-ray scattering revealed that the structure of both the blends and the graft copolymers contained highly ordered areas.

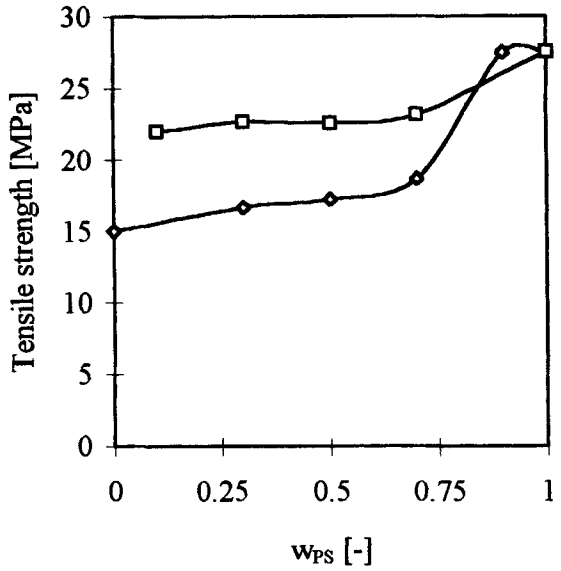

Fig. 10. Tensile strength as a function of PS ratio (PS blended with PS-g-starch). (Table 1), □: MAH-co-PS-g-starch, ◇: PS-g-starch.

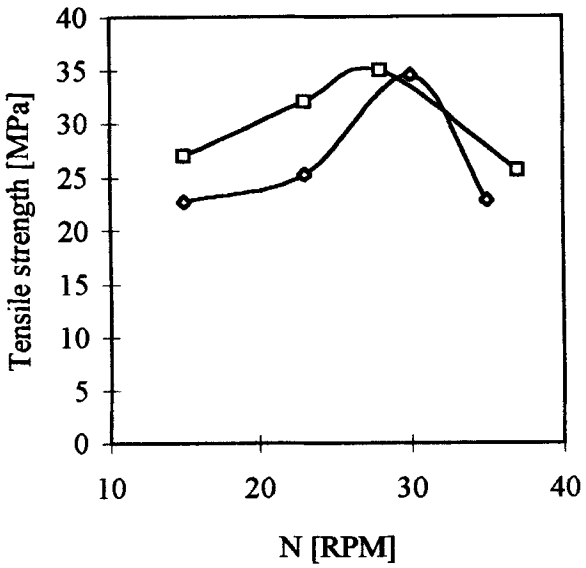

Fig. 9. Tensile strength as a function of the screw speed for the blend of PS with the grafted copolymer of starch and PS. (Table 1), □: MAH-co-PS-g-starch, M_w = 249,672 g mol^{-1}, ◇: PS-g-starch, M_w = 31,000 g mol^{-1}.

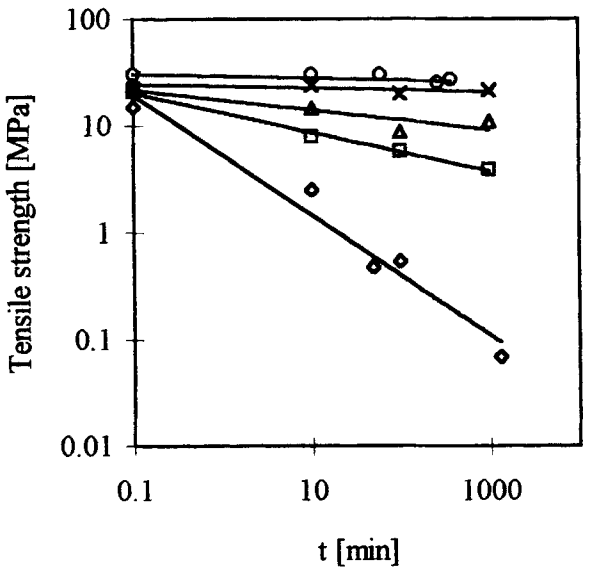

Fig. 11. Tensile strength as a function of the time the blend of PS with the PS-g-starch is soaked in water (Table 2). ◇: 2 wt% PS, □: 30 wt% PS, △: 50 wt% PS, x: 70 wt% PS, ○: 90 wt% PS.

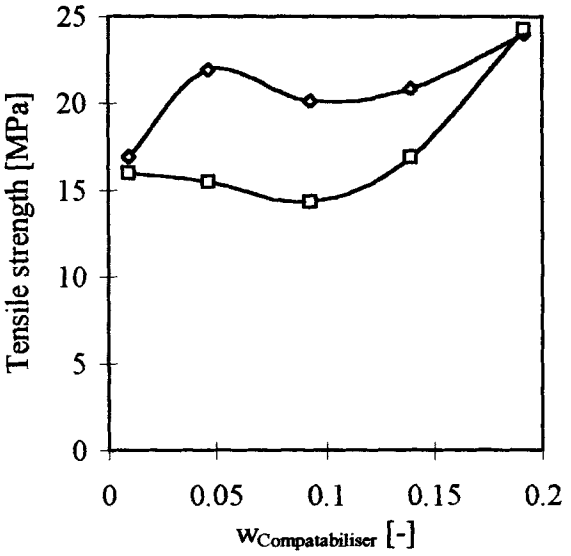

Fig. 12. Tensile strength as a function of the amount of compatibilizer present in blends of PS with starch (Table 3), □: PS-g-starch, ◇: MAH-co-PS-g-starch.

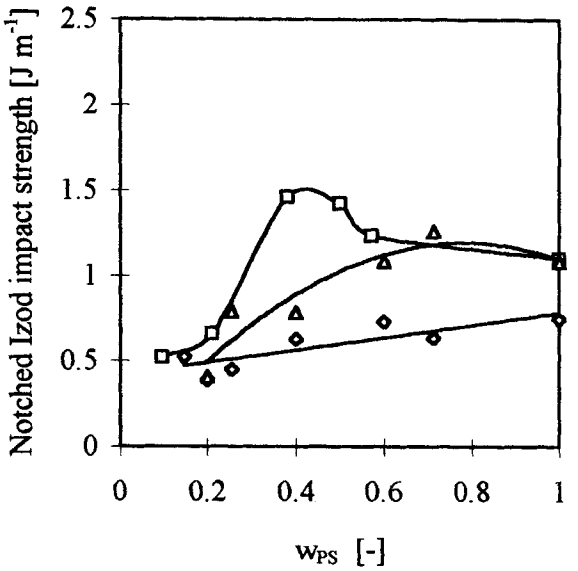

Fig. 14. Notched Izod impact strength as a function of the ratio PS in blends of PS, starch and PS-g-starch. (Table 3), ◇: M_w PS = 190 kg mol^{-1}, □: M_w PS = 220 kg mol^{-1}, △: M_w PS = 300 kg mol^{-1}.

NOMENCLATURE

a	Diameter	[m]
A	Interfacial area	[m^2]
B	Width	[m]
Ca	Capillary number	[-]
d	Diameter	[m]
L	Length	[m]
m	Amount of threads on a screw	[-]
n	Particle amount	[-]
N	Screw speed	[RPM]
Q	Throughput	[m^3 s^{-1}]
Ro	Radius	[m]
t	Time	[s]
V_c	C-shaped chamber volume	[m^3]
w	Weight fraction	[-]
η	Viscosity	[Pa s]
φ	Volume fraction	[-]
ν	Interfacial tension	[N m^{-1}]
γ	Shear rate	[s^{-1}]
Ψ	Viscosity ratio	[-]

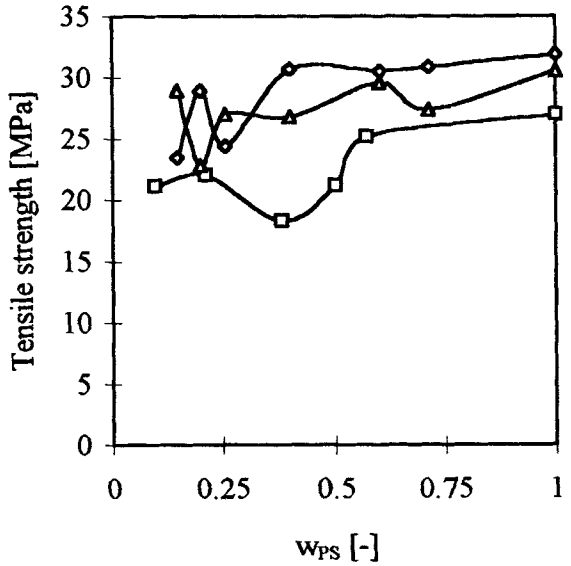

Fig. 13. Tensile strength as a function of the ratio PS in blends of PS, starch and PS-g-starch. (Table 3), ◇: M_w PS = 190 kg mol^{-1}, □: M_w PS = 220 kg mol^{-1} △: M_w PS = 300 kg mol^{-1}.

REFERENCES

1. G. F. Fanta, R. C. Burr, W. M. Doane, and C. R. Russell, *Macromoleculare Chemie*, **21**, 425 (1977).
2. O. B. Wurzburg, *Modified Starches and Properties*, Ch. 10, p. 149, CRC Press, Boca Raton Fla. (1986).
3. R. A. de Graaf and L. P. B. M. Janssen, *Polym. Eng. Sci.*, **40** (2000).
4. J. J. Elmendorp, in *Mixing in Polymer Processing*, C. Rauwendaal, ed., Marcel Dekker, New York (1991).
5. L. A. Utracki, *Polymer Alloys and Blends*, Hanser Publishers, Munich, Vienna, New York (1989).
6. P. H. M. Elemans, J. G. M. van Gisbergen, and H. E. H. Meijer, *Integration of Polymer Science and Technology*, Part 2, P. J. Lemstra and L. A. Kleintjens, eds., Elsevier Applied Science Publishers, London and New York (1988).
7. L. A. Utracki and Z. H. Shi, *Polym. Eng. Sci.*, **32**, 1824 (1992).
8. K. Y. Ng and L. Erwin, *Polym. Eng. Sci.*, **21**, 4 (1981).
9. G. M. Jordhamo, J. A. Manson, and L. H. Sperling, *Polym. Eng. Sci.*, **26**, 517 (1986).
10. G. I. Taylor, *Proc. R. Soc.*, (London), **A138**, 43 (1932).
11. J. J. Elmendorp, *Polym. Eng. Sci.*, **26**, 332 (1986).
12. H. P. Grace, *Chem. Eng. Comm.*, **14**, 225 (1982).
13. S. Tomotika, *Proc. Roy. Soc.*, (London), **A146**, 501 (1934).
14. S. Wu, *J. Polm. Sci.*, **34**, 19–30 (1971).

15. P. H. M. Elemans, *Phd thesis*, Eindhoven University, The Netherlands (1989).
16. G. Lammers and A. A. C. M. Beenackers, *Carbohydr. Polym.*, **24**, 55 (1994).
17. D. J. van Zuilichem and L. P. B. M. Janssen, in *Rheology*, Vol. 3, G. Astarita, G. Marrucci, and L. Nicolais, eds., Plenum Press, New York and London (1980).
18. K. D. Dolan and J. F. Steffe, *J. Textruder Stud.*, **21**, 265 (1990).
19. G. Pinto and Z. Tadmor, *Polym. Eng. Sci.*, **10**, 279 (1970).
20. R. A. de Graaf, M. Rohde, and L. P. B. M. Janssen, *Chem. Eng. Sci.*, **52**, 4345–4356 (1997).
21. D. R. Paul, in *Polymer Blends*, Vol. 2, D. R. Paul and S. Newman, eds., Academic Press: New York (1978).
22. C. E. Lock and D. R. Paul, *J. Applied Polym. Sci.*, **17**, 2791 (1973).
23. S. Thomas and R. E. Prud'homme, *Polymer*, **33**, 4260 (1992).
24. D. Heikens and W. Brentsen, *Polymer*, **18**, 69 (1977).
25. L. H. Sperling, *Polym. Eng. Sci.*, **25**, 517 (1985).